J Supercond Nov Magn (2013) 26:1909–1913
DOI 10.1007/s10948-012-2046-7

ORIGINAL PAPER

Intrinsic Optical Dichroism in the 2d Model of Chiral Superconducting State

Karol I. Wysokiński · James F. Annett · Balazs L. Györffy

Received: 7 November 2012 / Accepted: 3 December 2012 / Published online: 5 January 2013

Abstract Recently, we have found a new intrinsic mechanism of dichroism in chiral superconductors. It relies on the existence of many orbital character of the superconducting state as in Sr_2RuO_4. Using three orbital but a two-dimensional model relevant for superconducting strontium ruthenate, we calculate temperature T and frequency ω dependent ac Hall conductivity $\sigma_{xy}(\omega, T)$ for a number of parameters. In particular, we study the changes of σ_{xy} due to changes in the light frequency ω, spin–orbit coupling λ and effective interaction parameters U_{ij} between electrons occupying in-plane d_{2g} orbitals. Our calculations qualitatively agree with the measured Kerr rotation angle in Sr_2RuO_4 and have a potential to describe other superconductors.

Keywords Kerr effect · Optical dichroism · Chiral superconductor

1 Introduction

The understanding of the many puzzling properties of Sr_2RuO_4 superconductor has been a challenge for a long time [1]. In the normal state, this material seems to fulfill the criteria of a weakly correlated Fermi liquid [2–4]. Its superconducting state is fragile to the smallest number of impurities. Many of the thermodynamic properties including specific heat show power law temperature dependence requiring nodes in the order parameter. Other measurements indicate realization of the broken time reversed state [5]. In the bct crystal structure, reconciling consistently all of these properties requires a many band description of the system. The gaped but chiral order parameter of $k_x \pm ik_y$ variety exists on some of the bands and the order parameter with line nodes $(k_x \pm ik_y)\cos(k_z c/2)$ on the other bands. Many of these puzzling properties of the system have been accounted for by a three-dimensional, three-band model [6, 7]. Recently, we have shown that the existence of interorbital [8] components of the order parameter leads to natural explanation of the polar Kerr effect [9, 10] in strontium ruthenate and possibly other superconductors [11].

In this work, we analyze the dependence of the dichroic signal resulted from interorbital or interband coupling using simple three band model of 2d RuO plane. Such a model with "hidden quasi-one-dimensional superconductivity" has been recently introduced [12] and argued to lead to spin triplet ground state. Here, we adopt our previous tight binding energy spectrum and in accordance with [12] assume that the dominant interactions are between electrons occupying ruthenium d_{xz} and d_{yz} orbitals in the spin triplet channel. The weak interactions between carriers on d_{xy} orbitals lead to exponentially small gaps on the γ band. On the other hand, the interactions between carriers occupying d_{xz} and d_{yz} orbitals lead to both intraorbital and interorbital order parameters responsible for the Kerr effect.

2 Model and Approach

The Fermi surface of strontium ruthenate is known to appreciable details [13]. We shall use here our previous tight binding parameterization limited to the RuO plane. We neglect very weak hoppings leading to small corrugations of

K.I. Wysokiński (✉)
Institute of Physics, M. Curie-Skłodowska University,
Radziszewskiego 10, 20-031 Lublin, Poland
e-mail: karol@tytan.umcs.lublin.pl

J.F. Annett · B.L. Györffy
H. H. Wills Physics Laboratory, University of Bristol,
Tyndall Ave, Bristol BS8-1TL, UK

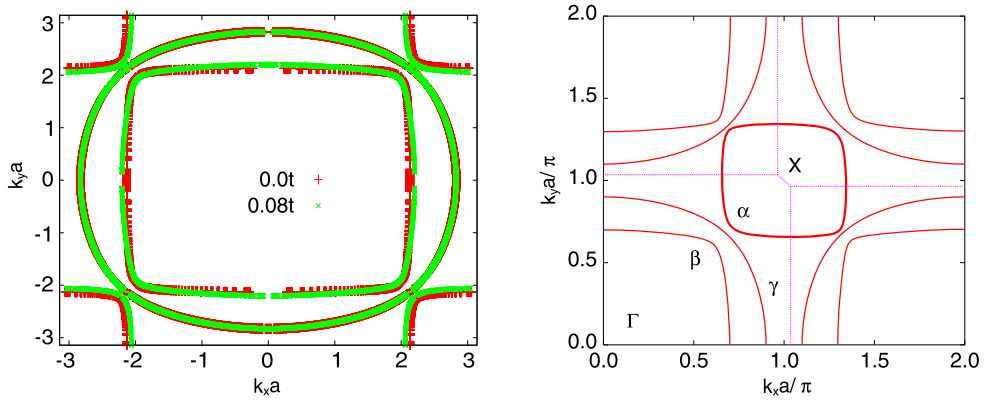

Fig. 1 The two-dimensional Fermi surface centered at the Γ point of the tetragonal Brillouin zone calculated for a band structure with $t_{ax} = 1.34$ and $t_{ay} = 0$ and for our standard band structure for Sr_2RuO_4 with $t_{ax} = 1.34$, $t_{ay} = 0.06t_{ax}$ (*left panel*). The same Fermi surface shown with the X point of the Brillouin zone at the center (*right panel*). In both cases, the hybridization parameter $t_{ab} \approx 0.1$. Note that the alpha Fermi surface sheet has only two-fold symmetry, because of the shape of the Brillouin zone boundary

the Fermi surface cylinders along the c crystallographic direction. However, we shall use all three partially occupied orbitals of Ru ions.

The normal state spectrum in the γ band derived from d_{xy} orbitals (called c orbitals in the following) reads

$$\varepsilon_{cc}(\mathbf{k}) = \varepsilon_{0c} - 2t(\cos k_x + \cos k_y) - 4t' \cos k_x \cos k_y, \quad (1)$$

while the α and β bands are derived from hybridize d_{xz} and d_{yz} orbitals. By symmetry, these orbitals do not hybridized with d_{xy}. Thus, the full normal state Hamiltonian in the orbital representation and neglecting spin–orbit coupling reads

$$\hat{H}_0(\mathbf{k}) = \begin{pmatrix} \varepsilon_{aa}(\mathbf{k}) & \varepsilon_{ab}(\mathbf{k}) & 0 \\ \varepsilon_{ab}(\mathbf{k}) & \varepsilon_{bb}(\mathbf{k}) & 0 \\ 0 & 0 & \varepsilon_{cc}(\mathbf{k}) \end{pmatrix}, \quad (2)$$

where, in units in which the in-plane lattice constant $a = 1$, $\varepsilon_{aa}(\mathbf{k}) = \varepsilon_{ab} - 2(t_{ax}\cos k_x + t_{ay}\cos k_y)$, $\varepsilon_{bb}(\mathbf{k}) = \varepsilon_{ab} - 2(t_{bx}\cos k_x + t_{by}\cos k_y)$ and $\varepsilon_{ab}(\mathbf{k}) = -4t_{ab}\sin k_x \sin k_y$. For the actual calculations, we use t as our energy unit. The other parameters fitted to the known experimental Fermi surface read: $t' = 0.45t$, $t_{ax} = t_{by} = 1.34t$, $t_{ay} = t_{bx} = 0.06t_{ax}$, $t_{ab} = 0.08t_{ax}$ and $\varepsilon_{0c} = -1.615t$, $\varepsilon_{ab} = -1.062t_{ax}$.

Our methodology is to solve the Bogoliubov–de Gennes equations

$$\begin{pmatrix} \hat{H}_0(\mathbf{k}) & \hat{\Delta}(\mathbf{k}) \\ \hat{\Delta}(\mathbf{k})^\dagger & -\hat{H}_0(\mathbf{k})^* \end{pmatrix} \begin{pmatrix} u_N(\mathbf{k}) \\ v_N(\mathbf{k}) \end{pmatrix} = E_N \begin{pmatrix} u_N(\mathbf{k}) \\ v_N(\mathbf{k}) \end{pmatrix} \quad (3)$$

self-consistently for eigenvectors $(u_N(\mathbf{k}), v_N(\mathbf{k}))^T$ and eigenenergies E_N at each $\mathbf{k}$ point of the two-dimensional Brillouin zone. The order parameter matrix is in general 6×6 matrix in the spin and orbital space. This is also true for $\hat{H}_0(\mathbf{k})$ in Eq. (2) if spin indices are taken into account. This extension is necessary if spin–orbit coupling is taken into account [6]. To obtain Hall conductivity, we use Fermi golden rule to calculate the polarization dependent absorption of electromagnetic radiation [14, 15], which is directly related to $\mathrm{Im}\,\sigma_{xy}(\omega, T)$ [16].

In the following calculations, we shall only consider the superconducting states with chiral symmetry as only these states are expected to lead to nonzero dichroic signal observed in strontium ruthenate. For the spin triplet superconductor, the orbital character of the order parameter is odd and we expect p-wave component to dominate. The order parameters have the following form

$$\Delta_{ij}(\mathbf{k}, T) = \Delta_{ij}^x(T)\sin(k_x a) + \Delta_{ij}^y(T)\sin(k_y a). \quad (4)$$

The complex coefficients $\Delta_{ij}^x(T)$ and $\Delta_{ij}^y(T)$ depend on temperature. a is the in-plane lattice constant.

3 Results

Let start the discussion of the results with presenting silent features of the underlying electron spectrum which Fermi surface consists of three sheets. They are shown in Fig. 1 in two different representations.

The Fermi surfaces were calculated assuming $t_{ay} = 0$ (left panel—plusses) and for $t_{ay} = 0.06t_{ax}$ (left panel—crosses). On the scale of the figure only small differences can be seen. Obviously, the spectrum of those bands calculated for $t_{ay} = 0$ shows more one-dimensional character. On the right panel, the same Fermi surface sheets are shown in the expanded Brillouin zone with X point at the center and Γ point in its corner to highlight the differences between α and β bands.

In Fig. 2, the temperature dependence of the various parameters $\Delta_{ij}^v(T)$ and the Hall conductivity $\mathrm{Im}\,\sigma_{xy}(\omega_0, T)$ are shown. The interaction parameters are assumed to be:

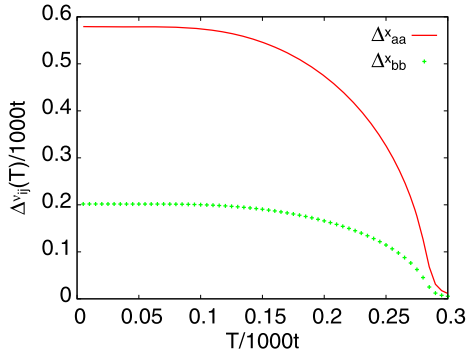

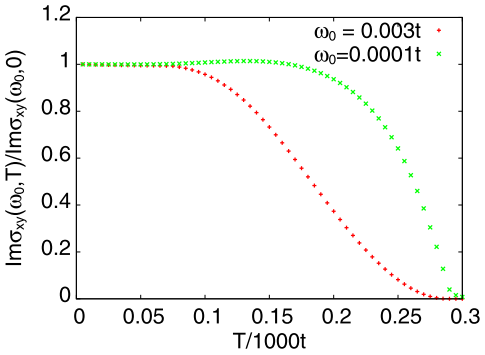

Fig. 2 The temperature dependence of the components of the order parameters $\Delta^{\nu}_{ij}(T)$ as defined in Eq. (4) (*left panel*) calculated with the interaction parameters $U_{aa} = U_{bb} = 0.6t$, $U_{cc} = 0.1t$, $U_{ab} = 0$ and no spin–orbit coupling. The *right panel* shows normalized Hall conductivity for the same model and for two different frequencies ω_0. Note the very small Hebel–Slichter like peak for the lower light frequency

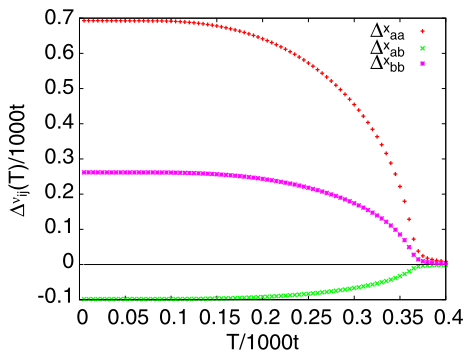

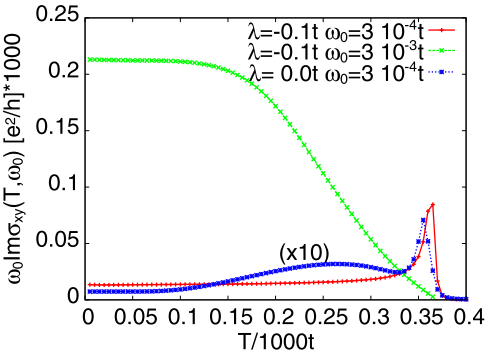

Fig. 3 The temperature dependence of the components of the order parameters $\Delta^{\nu}_{ij}(T)$ as defined in Eq. (4) (*left panel*) calculated for the interaction parameters $U_{ij} = 0.6t$ for $i, j = a, b$, and $U_{cc} = 0.1t$, $\omega_0 = 0.03t$ and spin–orbit coupling $\lambda = 0.0t$. *Right panel* shows $\mathrm{Im}\,\sigma_{xy}(\omega_0, T)$ in units of $e^2/\hbar$ for indicated values of λ and ω_0 with other parameters unchanged. Note the factor of 10 multiplying the curve obtained for $\lambda = 0$

$U_{aa} = U_{bb} = 0.6t$, $U_{cc} = 0.1t$, and $U_{ij} = 0.0$ for $i, j = a, b, c$. The only nonzero order parameters are those shown. Other order parameters are either exactly equal to those shown by symmetry or vanish. It is interesting to note the general symmetries between the Δ^x_{ij} and Δ^y_{ij} values in our model. They read $\Delta^x_{aa} = \pm i\Delta^y_{bb}$ and $\Delta^x_{ab} = \pm i\Delta^y_{ab}$. The symmetry with respect to exchange of k_x and k_y is also obvious in the Hamiltonian. The symmetries become more complicated if spin–orbit interaction is taken into account. The diagonal order parameters in Fig. 2 have different phases $\phi_{aa} \neq \phi_{bb}$ with the difference $\phi_{aa} - \phi_{bb} = \pi$. The same figure (right panel) shows the temperature dependences of the Hall conductivities normalized to their low T values calculated for two different frequencies of scattered light $\omega_0 = 0.003t$ and $\omega_0 = 0.0001t$. Close to T_c, $\mathrm{Im}\,\sigma_{xy}(T, \omega)$ calculated for lower frequency is strongly increased. We attribute this increase to coherence factors. It is typically observed for microwave frequencies of the order of the superconducting gaps or smaller. This increase is similar to the well-known Hebel–Slichter peak [17] and we shall use this name in the following. The zero temperature values of

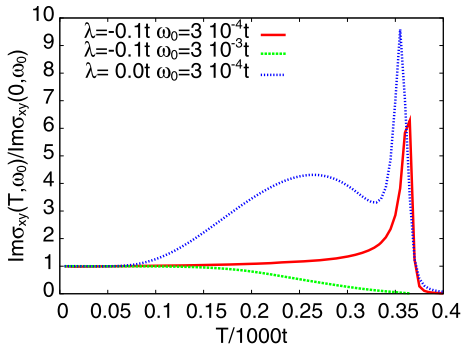

Fig. 4 The temperature dependence of the Hall conductivities normalized to their low T values and calculated for the same set of parameters as in Fig. 3

the $\omega_0\,\mathrm{Im}\,\sigma_{xy}$ shown in the figure read $2.1557\ 10^{-4}e^2/\hbar$ for $\omega_0 = 0.003t$ and $5.1712\ 10^{-6}e^2/\hbar$ for $\omega_0 = 0.0001t$. The peaks in the temperature dependence of $\mathrm{Im}\,\sigma_{xy}(\omega_0, T)$ are again shown in Fig. 4 for other set of parameters.

In Fig. 3 (left panel), we show the x components of the order parameters calculated for the couplings $U_{ij} = 0.6t$ for

$i, j = a, b$, and $U_{cc} = 0.1t$, and $\lambda = 0$. For these couplings the order parameter Δ_{cc} is exponentially small. Realistic value of the spin–orbit coupling $\lambda = -0.1t$ induces the cc component of the order parameter. For nonzero λ both order parameters and T_c (not shown) increase. The corresponding T dependences of the Hall conductivities calculated with $\lambda = 0$, $\omega_0 = 0.0003t$ and $\lambda = -0.1t$, $\omega_0 = 0.0003t$ and $\omega_0 = 0.00003t$ are shown in the right panel of the figure.

The most important influence of spin–orbit interaction on the superconductor at hand is the coupling of all three bands. Due to λ the superconducting order parameter is induced in the γ band and persists up to the common transition temperature T_c. Spin–orbit interaction also changes the symmetries between off-diagonal components of $\Delta_{ij}^{\nu;\uparrow\downarrow}$ (not shown). To understand such behavior one has to note that λ enters various matrix elements of the Hamiltonian with different signs, e.g., $\varepsilon_{ab}^{\uparrow\uparrow}(\mathbf{k})$ is supplemented by the term $-i\lambda$, while $\varepsilon_{ba}^{\uparrow\uparrow}(\mathbf{k})$ by $+i\lambda$. To the ac and bc components of the full spin dependent Hamiltonian matrix the terms $\pm\lambda$ are added. All this changes the effective Fermi level and the partial densities of states in all bands, and thus differently influences various components of the order parameters.

In the many orbital approaches, there are various contributions to the Hall conductivity. At zero temperature and for two orbital model $\mathrm{Im}\,\sigma_{xy}(\omega)$ is proportional[1] to the sum over wave vectors (suppressed in the formula below) of the expression containing *inter alia* the following terms

$$[(\mathbf{v_{bb}} - \mathbf{v_{aa}}) \times \mathbf{v_{ab}}]_z [\varepsilon_{ab}\,\mathrm{Im}(\Delta_{aa}^{*}\Delta_{bb}) + \varepsilon_{aa}\,\mathrm{Im}(\Delta_{bb}^{*}\Delta_{ab}) - \varepsilon_{bb}\,\mathrm{Im}(\Delta_{aa}^{*}\Delta_{ab})]. \quad (5)$$

For a nonzero Hall conductivity, it is enough to have two order parameters with nonvanishing imaginary part of their product. It may be two diagonal or one diagonal and one off-diagonal in orbital space. The asymmetry between elements $\mathbf{v_{bb}}$ and $\mathbf{v_{aa}}$ of velocities and nonvanishing $\mathbf{v_{ab}}$ is in this approach a necessary condition for nonzero dichroic signal. In the model at hand, we have checked that for $U_{aa} = 0$ the phase of Δ_{bb} and Δ_{ab} is the same and the Hall conductivity vanishes.

For some parameter sets, the Hall conductivity takes on large values. Its magnitude is obviously related to the frequency of light, inter-orbital couplings and other parameters. There seem to be no general rule for prediction if Hall conductivity will be large or small. The nonmonotonic dependence on temperature of $\mathrm{Im}\,\sigma_{xy}(\omega, T)$ of more complicated character than the single peak is also observed (see Fig. 3). Typically, the peak appears in the dichroic spectrum for microwave frequencies comparable or smaller than the gap function. This is in accordance with our previous 3d results and shows that to some extent the 2d model captures the physics of the real system. Of course, to have order parameters of symmetry compatible (in the group theoretical sense) with the underlying crystal structure with horizontal nodes one needs three dimensional spectrum.

In a general, three orbital case and at nonzero temperature each of the terms similar to those shown in Eq. (5) is additionally multiplied by the T dependent combination of Fermi functions and depends on T through the temperature dependence of the order parameters $\Delta_{ij}(T)$. The resulting expression depends on the frequency ω stemming from the conservation of energy and the eigenvalues of Bogoliubov–de Gennes equation. Being a sum of many terms, each of which depends on $\mathbf{k}$ it may also change sign as a function of frequency. This aspect makes it difficult to assign a particular orbital as the cause of dichroism and will be discussed elsewhere.

As stated earlier [8], the Hall conductivity changes sign with chirality (i.e., the sign in front of i in $k_x \pm ik_y$) of the state. The mere existence of the spin–orbit coupling is not enough to have nonzero Hall conductivity. However, both spin–orbit coupling and the magnetic field $\mathbf{B}$ breaking time reversal symmetry will induce Kerr signal even in one band model in analogy to magnetooptic effects [18]. The signal depends on the magnitude of the field.

In summary, we have studied in some details the novel mechanism of dichroism operating in multiorbital superconductors breaking time reversal symmetry. The main features agree with previous numerically more involved 3d calculations. In particular, the role of spin–orbit interaction has been elucidated and found to lead to qualitative and quantitative changes of the temperature dependence of the Hall conductivity. We also established the existence of the Hebel–Slichter like coherence peak in a 2d model.

Acknowledgements This work has been partially supported by the Ministry of Science and Higher Education grant No. N N202 2631 38.

[1] Similar ideas of interband contribution to the Kerr effect as in [8] have been developed by Taylor and Kallin [9]

References

1. Mackenzie, A.P., Maeno, Y.: Rev. Mod. Phys. **75**, 657 (2003)
2. Pchelkina, Z.V., Nekrasov, I.A., Pruschke, Th., Sekiyama, A., Suga, S., Anisimov, V.I., Vollhardt, D.: Phys. Rev. B **75**, 035122 (2007)
3. Singh, D.J.: Phys. Rev. B **77**, 046101 (2008)
4. Pchelkina, Z.V., Nekrasov, I.A., Pruschke, Th., Suga, S., Anisimov, V.I., Vollhardt, D.: Phys. Rev. B **77**, 046102 (2008)
5. Luke, G.M., Fudamoto, Y., Kojima, K.M., et al.: Nature **394**, 558 (1998)

6. Annett, J.F., Litak, G., Gyorffy, B.L., Wysokinski, K.I.: Phys. Rev. B **66**, 134514 (2002)
7. Annett, J.F., Gyorffy, B.L., Litak, G., Wysokinski, K.I.: Eur. Phys. J. B **36**, 301 (2003)
8. Wysokinski, K.I., Annett, J.F., Györffy, B.L.: Phys. Rev. Lett. **108**, 077004 (2012)
9. Taylor, E., Kallin, C.: Phys. Rev. Lett. **108**, 157001 (2012)
10. Xia, J., Maeno, Y., Beyersdorf, P.T., et al.: Phys. Rev. Lett. **97**, 167002 (2006)
11. Kapitulnik, A., Xia, J., Schemm, E., et al.: New J. Phys. **11**, 055060 (2009)
12. Raghu, S., Kapitulnik, A., Kivelson, S.A.: Phys. Rev. Lett. **105**, 136401 (2010)
13. Bergemann, C., Julian, S.R., Mackenzie, A.P., NishiZaki, S., Maeno, Y.: Phys. Rev. Lett. **84**, 2662 (2000)
14. Capelle, K., Gross, E.K.U., Gyorffy, B.L.: Phys. Rev. Lett. **78**, 3753 (1997)
15. Capelle, K., Gross, E.K.U., Gyorffy, B.L.: Phys. Rev. B **58**, 473 (1998)
16. Bennett, H.S., Stern, E.A.: Phys. Rev. **137**, A448 (1965)
17. Hebel, L.C., Slichter, C.P.: Phys. Rev. **107**, 901 (1957)
18. Ebert, H.: Rep. Prog. Phys. **59**, 1665 (1996)